

PAPER • OPEN ACCESS

Modeling of the process of solar drying of grapes in indirect type installations with natural air convection

To cite this article: Jura Jumaev *et al* 2023 *J. Phys.: Conf. Ser.* **2573** 012043

View the [article online](#) for updates and enhancements.



244th ECS Meeting

Gothenburg, Sweden • Oct 8 – 12, 2023

Register and join us in
advancing science!

Learn More & Register Now!



Modeling of the process of solar drying of grapes in indirect type installations with natural air convection

Jura Jumaev, Salim Ibragimov and Shavkat Mirzaev

Bukhara State University, Bukhara, Uzbekistan

E-mail: j.jumaev @buxdu.uz

Abstract. The paper models the process of natural convection of an indirect type dryer mathematically for the accumulation and absorption of heat which uses water. The data from the experiment conducted by the authors of the work is used as the initial data. The Reynolds equations and the temperature distribution equations are used for the mathematical model considering the Boussinesq hypothesis. The SIMPLE control volume method is used in the paper for the difference approximation of the initial equations. The temperature and velocity fields in the drying chamber are determined. It is revealed that the maximum speed in this mode is reached in the upper part of the dryer and it will be equal to 0.02-0.03 m/s.

1. Introduction

The Republic of Uzbekistan is a major producer of agricultural products and therefore the country pays special attention to their deep processing.

According to the Decree of the President of the Republic of Uzbekistan for № IIII-4406 dated July 29, 2019 "On additional measures for deep processing of agricultural products and further development of the food industry" provides for the development of the food industry, in particular deep processing of raw materials with the involvement of cooperatives, dehqan (peasant) farms, farmers and small enterprises [1]. At the same time, the most important task of processing plant raw materials is to increase the yield of finished products while preserving useful substances.

One of the methods for long-term preservation of the product with its useful substances is drying.

Solar drying is considered a traditional method and has been used for many years by many farms in developing and developed countries as a method of preserving food products. Indirect solar dryers use an enclosed space in which the food product is located.

Indirect type solar dryers are divided into natural convection (passive type) and forced convection (active type). Solar dryers with natural convection are easy to manufacture and have a low cost.

Many works have been devoted to modeling solar systems for various purposes [2-5].

The study of the authors [3] is focused on the analysis of the temperature profile, heat transfer characteristics and thermal efficiency of a flat plate solar collector (FPSAC) at various mass airflows. Also, with the help of multivariate analysis of the study, relationships were established among several other variables of thermal characteristics.

Experiments were carried out in an unloaded mode and in the open air under the conditions of natural and forced air convection in the collector of a solar dryer.



An analysis of the principal parametric components made it possible to visualize the association among solar intensity, temperature in various reservoir elements, heat transfer coefficients, thermal efficiency and time of day. The results show that the useful heat gain, the heat transfer coefficient of the air and the thermal efficiency of the collector do not strongly depend on the intensity of solar radiation.

In the work [4], a solar dryer with natural convection of an indirect type was developed. Here, the air heater is designed in such a way as to be able to insert various storage materials under the absorbent plate to improve the drying process. Sand is used as a material for storing heat. Thus, the accumulation and storage of heat reduced the drying process by 12 days.

In [5], a solar dryer with indirect forced convection equipped with a sensitive heat accumulating material was developed. We came to the conclusion that the dryer integrated with the heat storage material allows maintaining a constant air temperature inside the dryer.

The closed form of the device is optimal for the preservation of useful substances. In order to dry the product in a closed device, it is necessary to bring warm air to it.

There are several types of solar dryers that are currently being used. In water devices, the supply of warm air is carried out through solar collectors [6], where stones are used as a heat accumulator.

Studying the possibilities of water heating installations, we came to the conclusion that the flow of warm air can be obtained with a natural solar water heater.

Solar convection dryer with water heater was manufactured and installed by us in the scientific laboratory of the Department of "Heliophysics and Renewable Energy Sources" of Bukhara State University, Bukhara, Republic of Uzbekistan. At the same time, the dimensions of this dryer are selected from the consideration that its dimensions are small, that it can be transported easily. In order to theoretically investigate the process inside the dryer, a mathematical model was compiled.

2. Experimental part

A general view of the dimensions and points of taking the experiment of such a device is shown in figure 1, and its general scheme is shown in figure 2.

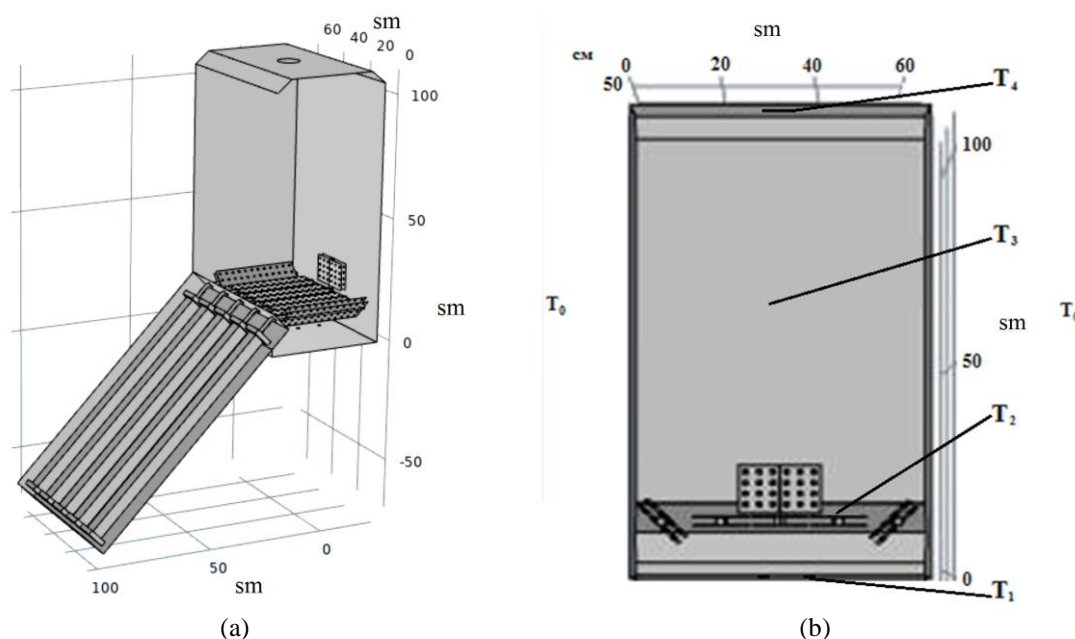


Figure 1. General view of the solar dryer, a) internal view, b) points of taking the experiment.

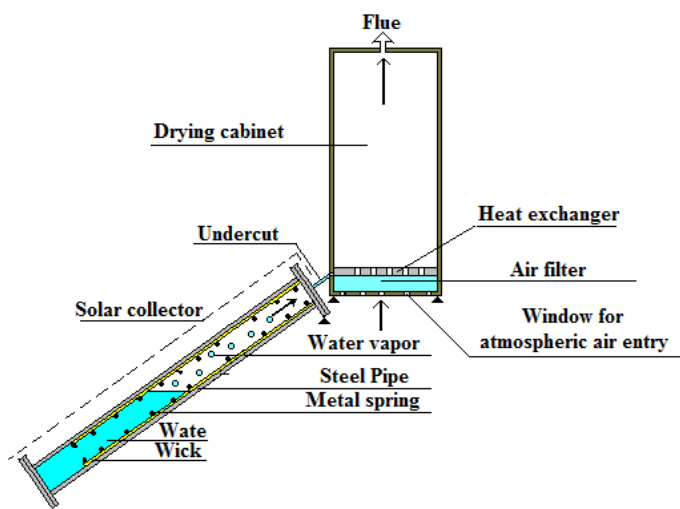


Figure 2. Diagram of a solar dryer.

The presented heat pipe (HP) is a countercurrent hermetic system, which consists of a steel pipe (one end of the system) and a flat metal heat exchanger (the second end of the system). There is water in the pipe cavity in the volume of 1/3 or 2/3, the wick is made of knitted material and a spring made of metal wire is installed along the inner wall of the pipe to strengthen the wick. One end of the HP system (heater) is surrounded by a flat solar collector in which the heat is isolated from the environment. This end of the HP system is heated by solar radiation, i.e. solar radiation passing through the surface of the transparent surface (cover) of the solar collector falls on the outer surface of the steel pipe, heats the water inside the HP and causes water evaporation. Water vapor passing through the subheadings enters the opposite end (the second end) of the HP system. The second end consists of a metal flat heat exchanger, which has a low temperature, which causes condensation of water vapor, accompanied by the release of heat. The second end of the HP system is installed inside the drying chamber.

Thus, due to the difference in densities inside the drying chamber, a heat flow occurs. An experiment of the heating process during the flight day was carried out in a collector, a drying chamber without food products. To obtain experimental data, certain points in the device are selected (figure 1 b), the numerical values of which are given in table 1. With these data in mind, in order to understand the convection process inside the closed region, numerical modeling was performed.

Table 1. Experimentally measured temperature data.

Time	T ₁	T ₂	T ₃	T ₄	T ₀
10:00	38.81	45.38	41.69	40.81	36.3
11:00	39.13	47.94	43.94	42.19	36.6
12:00	39.44	49.06	44.56	42.56	37.2
13:00	40.31	51.25	46.56	44.06	37.8
14:00	40.63	51.44	48.56	43.19	37.2
15:00	40	52.75	47.81	44.5	37.8
16:00	44	56	52	46.81	41
17:00	45.69	55.19	52.56	47.81	41.12
18:00	40.63	50.06	47.69	42.13	39.98
19:00	38.06	42.63	41.63	37.06	37.11
7:00	22.31	27.5	23.75	22.75	22.12

3. Methods

As can be seen from figure 1, the drying chamber is closed and a round hole in the middle of the upper lid in the size of 0.1 m² is inserted for the air outlet. Thus, when heated from below, vortices appear in the chamber, a turbulent flow regime may appear. It is possible to estimate the flow mode by calculating the Grashof number:

$$Gr = \frac{g \cdot \beta \cdot \Delta T \cdot L^3}{\nu_m^2} = \frac{g \cdot \beta \cdot (T_h - T_o) \cdot L^3}{\nu_m^2} = 4,3 \cdot 10^9 \quad (1)$$

The reasoning behind the fact that when the convective flow turns into turbulent is different. For example, according to the authors [7], at $Gr \cdot Pr > 10^{10}$ the gas flow is assumed to be turbulent. In our case, if the Prandtl number is taken to be $Pr = 0.7$, then we get $Pr \cdot Gr = 3 \cdot 10^9$. According to the authors [8], at $Gr \cdot Pr > 10^9$, the convective gas flow can be assumed to be turbulent. The Grashof number calculated by the formula (1) corresponds to a critical value, so turbulent stresses can also be calculated.

Turbulent flow can be represented as a set of vortices rotating in different directions and in different planes. Large clots turn into small clots, and small clots, i.e. clots whose size slightly exceeds the free path of the molecule, convert their energy into viscous thermal energy. Initially, this process was developed by A.N. Kolmogorov and called the energy cascade.

Taking into account the correlation mentioned above between laminar and turbulent air movements, a mathematical model was developed for the direct dependence of the longitudinal temperature distribution on the air velocity in the ducts of a solar air collector with recessed air ducts.

Bearing in mind the above, the Reynolds equations and the temperature distribution equations, taking into account the Boussinesq hypothesis, can be written as follows [7-9]

$$\left\{ \begin{array}{l} \frac{\partial u_i}{\partial t} + \frac{\partial(u_i u_j)}{\partial x_j} = -\frac{\partial p}{\rho \partial x_i} + \frac{\partial}{\partial x_j} \left((\nu + \nu_t) \frac{\partial u_i}{\partial x_j} \right) + g \beta (T - T_0), \\ \frac{\partial T}{\partial t} + u_i \frac{\partial T}{\partial x_j} = \frac{\partial}{\partial x_j} \left((K + K_t) \frac{\partial T}{\partial x_j} \right) \\ \frac{\partial u_j}{\partial x_j} = 0, \quad (i, j = 1, 2, 3) \end{array} \right. \quad (2)$$

Here u_i - is the air flow velocity; p - is the hydrostatic pressure; T - is the temperature; g – is the acceleration of gravity; β is the thermal coefficient of volumetric expansion; ν, ν_t - is the laminar and turbulent viscosity components; $k = \frac{\nu}{Pr}, k_t = \frac{\nu_t}{Pr}$, where Pr, Pr_t - are the Prandtl numbers for laminar and turbulent flow modes.

In the Reynolds equation above, unknown terms are formed, called Reynolds stresses.

Currently, there are many different semi-empirical models for determining Reynolds stresses.

The Spalart-Allmaras model.

The Spalart-Allmaras model was developed specifically for aerospace applications involving flows confined by walls, and it has been shown that it gives good results for boundary layers, even those subject to negative pressure gradients [10].

In our work, the Spalart-Allmaras model was used to determine the turbulent viscosity, which has the form:

$$\frac{\partial \tilde{\nu}}{\partial t} + u_j \frac{\partial \tilde{\nu}}{\partial x_j} = C_{b1}(1 - f_{t2})\tilde{S}\tilde{\nu} - \left[C_{w1}f_w - \frac{C_{b1}}{k^2} f_{t2} \right] \left(\frac{\tilde{\nu}}{d} \right)^2 + \frac{1}{\sigma} \left[\frac{\partial}{\partial x_j} \left((\nu + \tilde{\nu}) \frac{\partial \tilde{\nu}}{\partial x_j} \right) + C_{b2} \frac{\partial \tilde{\nu}}{\partial x_j} \frac{\partial \tilde{\nu}}{\partial x_j} \right] \quad (3)$$

Here the turbulent exchange coefficient is defined as follows:

$$\nu_t = \tilde{\nu} f_{\nu 1}$$

Additional functions and constants of the model are given in [10]:

In the work, after dimensionalization of the basic equations, the control volume SIMPLE method was used for difference approximation [11]. The integration was carried out in time steps $\Delta t < 0.001$. The simulation was started from time $t=0$ s and was modeled up to the time given in the experiment using a fixed Courant number 1.

1623235 points were used in the work, the grid was thickened near the perforated plates.

For the initial and boundary conditions, experimental data from table 1 are accepted. The problem is considered three-dimensional in a non-stationary state.

4. Results and discussion

Figure 3a shows the velocity field in one vertical plane and throughout the drying chamber. The temperature data in the scale is given in kelvins. As can be seen from the figure, with the appropriate selection of the desired plates, the temperature is evenly distributed throughout the drying chamber. The maximum temperature adheres to almost the entire area.

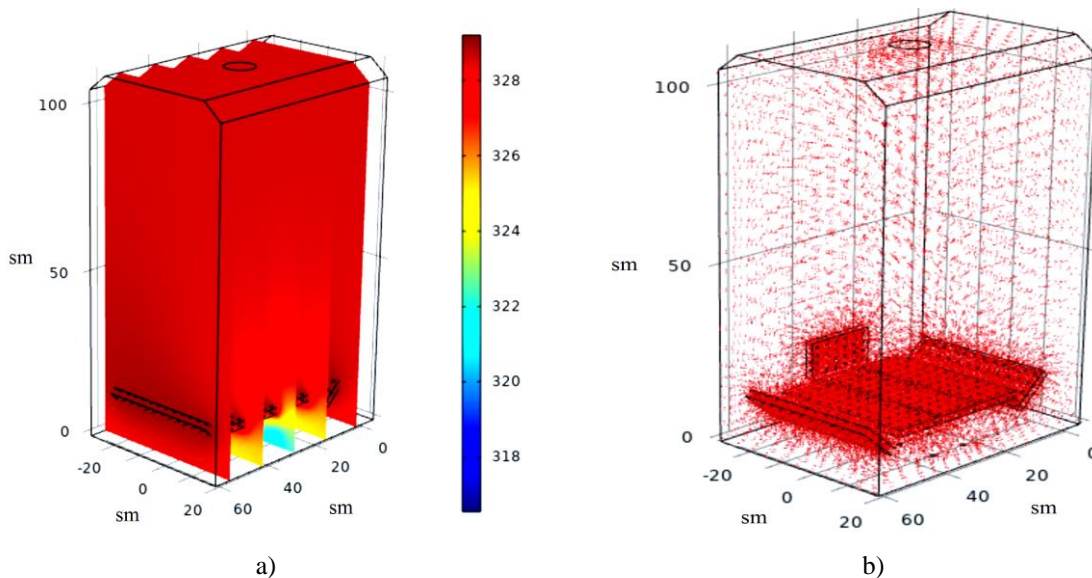


Figure 3. Temperature distribution (in kelvins) in one vertical plane and over the entire area: a) the velocity field in one vertical plane and throughout the drying chamber; b) isolines of the temperature directions along the drying chamber

Figure 3b shows the isolines of the temperature directions along the drying chamber. From these isolines, it can be concluded that the temperature flow reaches the entire area of the drying chamber.

Figure 4a shows the velocity fields in the drying chamber. As can be seen from the scale, the speed is the same in almost the entire region, and is approximately equal to 0.004-0.006 m/s. Only near the upper hole, due to a decrease in the area, there is a slight increase.

Figure 4b shows the isolines of the speed along the drying chamber. As can be seen from the figure, the velocity flow reaches all areas of the drying chamber.

Figure 5 shows the calculated temperature values in comparison with those experimentally measured at the points of the freezer.

The relative error between the theoretically found values and the experiment is found by the formula

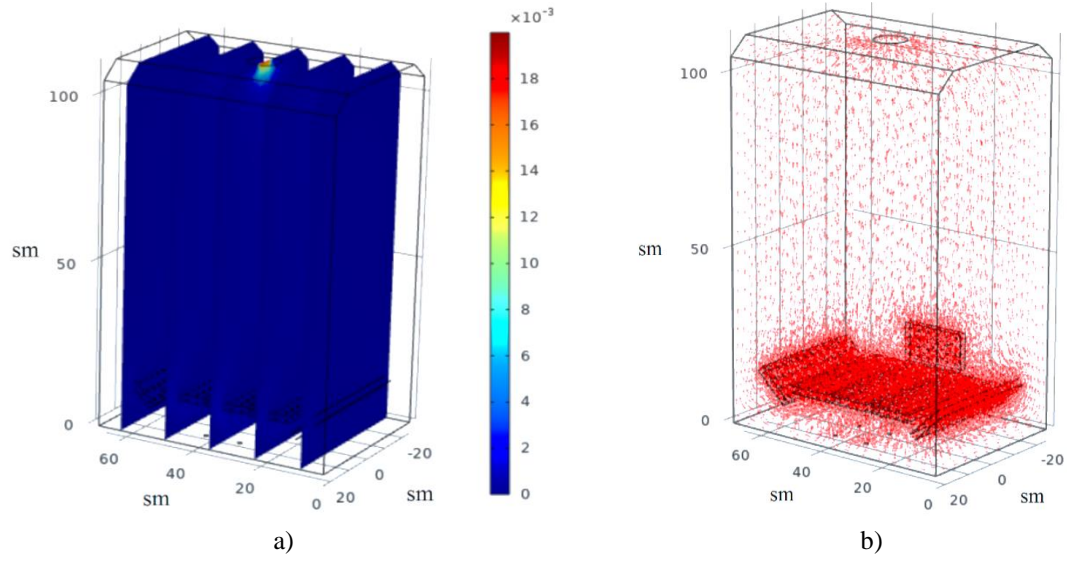


Figure 4. The field (a) and the isolines (b) of the speed along the drying chamber.

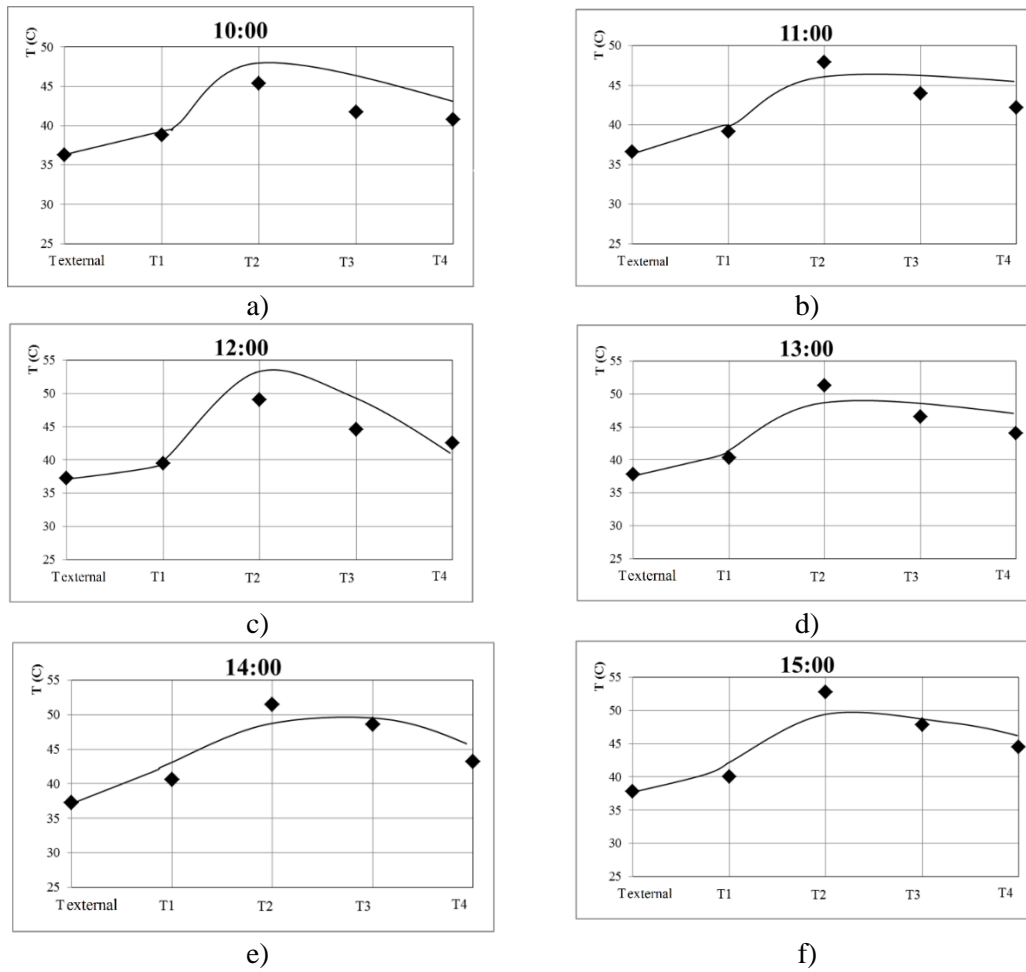


Figure 5. Comparison of experimental and theoretical data at selected points from figure 1b during the day. a) 10:00; b) 11:00; c) 12:00; d) 13:00; e) 14:00; f) 15:00.

$$\bar{A} = \frac{1}{n} \frac{\sum_{i=1}^n |y_i - \bar{y}_i|}{y_i}$$

where y_i – is the experimental values, \bar{y}_i – is the theoretically found values, n – is the number of experimental points.

According to calculations, for all experiments, the relative error does not exceed 6%. This means that the model describes the convection process inside the dryer well.

5. Conclusion

In this work, the process of free convection is mathematically modeled for a designed water dryer. The initial data were obtained by conducting an experiment in this drying chamber. According to the initial data, the Grashof number was calculated, which showed that turbulent flow can occur in this drying chamber.

Based on this, a system of differential equations for the unsteady flow of natural air convection is chosen using the law of conservation of mass, momentum, and energy in the Boussinesq approximation, as well as the Spalart-Allmaras model for determining turbulent stresses. To solve the problem, the SIMPLE control volume method was applied. The integration was carried out in time steps $\Delta t < 0.001$. The simulation was started from time $t=0$ s and was modeled up to the time given in the experiment.

The dependence of the air temperatures at the entrance and exit from the freezer, as well as in the surface of the heat source on the measurement time was established, experimental and calculated data were compared, that is, a clear picture of the relationships between variables was established and compared based on multidimensional analysis methods. To evaluate the effectiveness of the obtained model, an average approximation error of 6% was revealed. The price of the model also increases the level of reliability in the production of hot (warm) air with natural circulation in such drying chambers.

References

- [1] Decree of the President of the Republic of Uzbekistan dated July 29, 2019 No. PP-4406 “on additional measures for the deep processing of agricultural products and the further development of the food industry”
- [2] Duffie J A and Beckman W A 2013 *Solar Engineering of Thermal Processes* (New Jersey)
- [3] Poonam Rani and Tripathy P P 2020 *Solar Energy* **211** 464-77
- [4] El-Sebaï A A, Aboul-Enein S, Ramadan M R I and El-Gohary H G 2002 *Energy Conversion and Management* **43** 2251-66
- [5] Mohanraj M and Chandrasekar P 2009 *Journal of Engineering Science and Technology* **4(3)** 305-14
- [6] Mirzaev Sh, Kodirov J and Khamraev S I 2022 *IOP Conf. Series: Earth and Environmental Science* **1070** 012021
- [7] Schlichting G 1974 *Theory of the boundary layer* (M: Science)
- [8] Gebhart B, Jaluria J, Mahajan R L and Sammakia B 1991 *Free-convective flows, heat and mass transfer* (M.: Mir)
- [9] Jumayev J, Shirinov Z and Kuldashev H 2019 Computer simulation of the convection process near a vertically located source *International conference on information Science and Communications Technologies (ICISCT) 4-6 november. 2019. Tashkent. Conference Proceedings* pp 635-8
- [10] Khamidov R and Mamatkarimov O 2022 *Instruments and Experimental Techniques* **65(2)** 314-7
- [11] Patankar Suhas V and Spalding D Brian 1972 *International Journal of Heat Mass Transfer* **15** 1787-806